International Journal of Fluid Mechanics Research, Vol. 32, No. 4, 2005

Modelling Convection Heat Transfer in a Rotating Fluid in a Thermally-Stratified High-Porosity Medium: Numerical Finite Difference Solutions[†]

O. Anwar Bég
Leeds College of Building, Leeds Metropolitan University
North Street, Leeds, LS2 7QT, UK, email: OBeg@lcb.ac.uk

H. S. Takhar
Engineering Department, Manchester Metropolitan University
Oxford Rd., Manchester, M5, UK

Tasveer A. Bég
Engineering Mechanics Researcher & Consultant
18 Milton Grove, Manchester M16 OBP, England, UK

A. J. Chamkha
Mechanical Engineering Department
The Public Authority for Applied Education and Training
PO Box 42325, Shuweikh, 70654, Kuwait

G. Nath
Mathematics Department, Indian Institute of Science, Bangalore, India

Rui Majeed
Biomedical Scientist, Kashmir Gardens, Darnall, Sheffield, UK

The convective heat transfer flow in a rotating fluid over a vertical plate in a non-Darcian thermally-stratified high-porosity medium is studied. The governing partial differential equations for momentum and energy are solved numerically using Blottner's finite-difference method. The effects of Rossby number and various thermal parameters on velocities, temperature, skin friction and Nusselt number are presented graphically and discussed at length. The flow and temperature fields are strongly influenced by the thermal stratification, porosity, inertia and Rossby number, whereas they demonstrate a weak dependence on the permeability parameter. Beyond a critical value of the Rossby number ($\mathrm{Ro} \geq 0.5$) flow reversal occurs in the X-component of the velocity. Other flow phenomena including primary and secondary flows are discussed. The problem finds applications in rotating industrial and geophysical systems.

* * *

[†]Received 21.06.2005.

ISSN 1064-2277

Introduction

The topic of rotating flows has received wide interest in modern fluid dynamics research. Excellent treatises on this subject with applications in geophysics and planetary sciences have been in the literature since the early 1950s. These include the seminal studies by Lyttleton [1] and later Greenspan [2]. The coupled effects of heat transfer on rotational hydrodynamics has largely been inspired by applications in chemical engineering and manufacturing processes in the chemical industry. Simultaneous rotational and buoyancy effects in thermal convection abound in the modeling of process devices, centrifugal operations, catalytic reactors as well as in geothermal energy systems. Early studies include those by Dorfman [3] and Krieth [4], the latter presenting an excellent article on rotating surface convection heat transfer. Rotem and Classen [5] studied the thermal convection in the vicinity of a rotating horizontal disk. Suwono [6] examined the mixed convection for rotating round-nosed bodies with vertical axes, providing numerical solutions for the case of a rotating sphere. Asymptotic studies of higher order heat transfer from a sphere were reported by Takhar and Whitelaw [7]. More recently Hossain and Takhar [8] studied the effects of radiative heat transfer on mixed convection on rotating bodies. Naroua et al [9] presented a finite element analysis of natural convection flow in a rotative fluid with radiative heat transfer. Deka et al [10] studied the flow past an accelerated horizontal plate in a rotating fluid.

Considerable research has also been directed towards examining thermal convection flows in porous media with a variety of thermophysical effects. Pop, Soundalgekar and Takhar [11] studied the dispersion of a solute in a Darcian porous medium channel with homogenous and heterogenous chemical reaction. Takhar et al [12] examined the transient hydrodynamic flow in porous medium between two infinite parallel plates in relative motion. Raptis and Takhar [13] investigated the forced flow and species transfer in a porous medium. In many geophysical situations the temperature of the porous medium varies with depth i. e., the medium is thermally stratified. It is important to incorporate this effect in the mathematical simulation model as it can have a bearing on heat transfer rates. This led Takhar and Pop [14] to study the free convection from a vertical flat plate to a thermally stratified porous medium. In this analysis however only a Darcian flow model was incorporated. When higher velocities are experienced in porous systems the Darcy flow model is inadequate as it cannot capture inertial effects. Many authors have therefore adopted a Darcy – Forcheimmer drag force model in transport modeling of porous media. Vafai and Tien [15] were amongst the first researchers to apply the Darcy – Forcheimmer model to convection in porous media. They also incorporated the Brinkman vorticity diffusion effects which take place at the boundary. Kumari, Takhar and Nath [16] later applied a non-Darcy boundary layer model to study the free convection from two-dimensional and axi-symmetric bodies of arbitrary shape in a saturated porous medium. They extended this work to mixed convection flows [17]. Takhar, Soundalgekar and Gupta [18] applied the Darcy – Brinkman model in their study of mixed convection past a hot vertical plate embedded in a porous medium. Gorla and Takhar [19] used a shooting method to numerically simulate the combined convective heat transfer from a plate in a saturated porous medium. Takhar and Bég [20] were among the first researchers to study the hydromagnetic non-Darcy mixed convection flow in a saturated porous medium. Bég et al [21] analyzed the radiation effects on non-Darcy non-gray gas convection in a porous medium using the Keller-Box implicit difference scheme. More recently Bég et al [22] investigated the viscoelastic convection in a Darcy – Brinkman – Forcheimmer porous medium. The specific case of high porosity medium was considered by Takhar, Chamkha and Nath [23] for the natural convection on a vertical cylinder embedded in a thermally stratified porous medium. In the present problem we shall study the effects of rotational parameter (Rossby number), thermal stratification parameter, porosity and permeability parameter on the thermal and

velocity fields in a rotating porous medium regime. Certain porous materials e. g., foam metals and fibrous insulations, possess a high porosity (with a value between 0.9 and 0.95). Thermal stratification occurs in cooling ponds, lakes, solar hydro-collection systems and also in atmospheric regimes. If a vertical surface is part of the enclosure, the ambient temperature of the fluid will be stratified. For stable thermal stratification, the temperature in the ambient fluid increases with height.

1. Mathematical Model

The problem to be examined is illustrated below in Fig. 1. Consider a Cartesian coordinate system (x, y, z) rotating uniformly with the fluid. The heated vertical plate is embedded in a highly porous medium and is aligned along the x direction in the xy plane. Fluid is rotating with a constant angular velocity, Ω, about the z-axis which is horizontal and normal to the plate surface. Gravity acts in the negative x-direction. Fluid properties are assumed to be constant except the density variation which gives rise to buoyancy forces. The fluid rotation gives rise to a secondary flow which makes the flow field three-dimensional, having velocity components u, v, and w in the x, y and z-directions, respectively. Since the plate is orientated along the x-axis, the flow and temperature fields are independent of y and depend on x and z only. We have considered herein non-Darcy effects which incorporate inertia, boundary and convective effects using volume-averaged principles and empirical results [24]. The porous medium is assumed to be homogenous and isotropic so that only one permeability is required to model it. Under the above assumptions along with the usual Boussinesq approximations the boundary layer equations based on the conservation of mass, momentum and energy incorporating non-Darcian effects governing the free convection flow of a rotating fluid over a vertical plate in a rotating coordinate system can be expressed as:

Conservation of Mass:

$$\frac{\partial u}{\partial x} + \frac{\partial w}{\partial z} = 0, \tag{1}$$

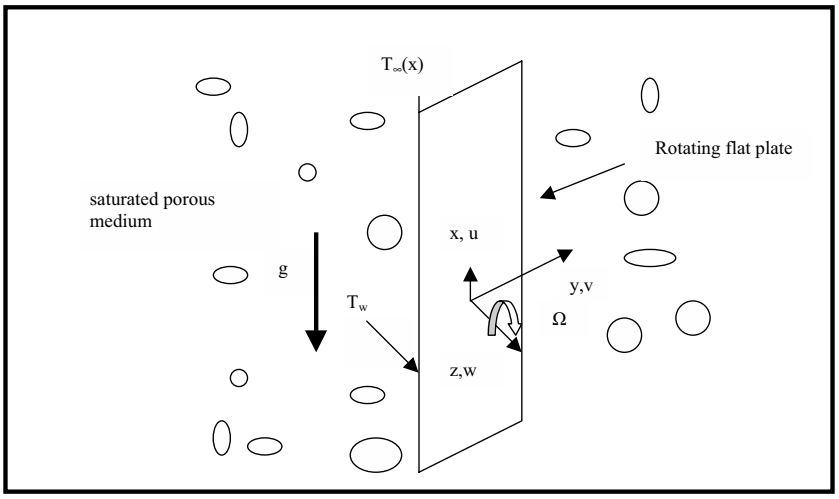

Fig. 1. Rotating convection in a thermally-stratified porous medium.

Momentum:

$$\varepsilon^{-1}\left[u\frac{\partial u}{\partial x}+w\frac{\partial u}{\partial z}-2\Omega v\right]=\varepsilon^{-1}\nu\frac{\partial^2 u}{\partial z^2}-\frac{\nu}{K^*}u-C^*u^2+g\beta(T-T\infty), \tag{2}$$

$$\varepsilon^{-1}\left[u\frac{\partial v}{\partial x}+w\frac{\partial v}{\partial z}+2\Omega u\right]=\varepsilon^{-1}\nu\frac{\partial^2 v}{\partial z^2}-\frac{\nu}{K^*}v-C^*v^2. \tag{3}$$

Energy (Heat):

$$u\frac{\partial T}{\partial x}+w\frac{\partial T}{\partial z}=\alpha_e\frac{\partial^2 T}{\partial z^2}\,. \tag{4}$$

Boundary Conditions:

$$u(x,0)=v(x,0)=w(x,0)=0,\qquad T(x,0)=T_w, \tag{5}$$

$$u(x,\infty)=v(x,\infty)=0,\qquad T(x,\infty)=T\infty(x), \tag{6}$$

$$u(0,z)=v(0,z)=0,\qquad T(0,z)=T_0, \tag{7}$$

where u, v and w are the x-, y- and z-direction velocities respectively; K^* denotes the permeability parameter; C^* is the Forcheimmer (inertial) coefficient, ε is the porosity of the porous medium; α_e is the effective thermal diffusivity of the composite fluid-porous medium; g is gravitational acceleration; β denotes the volumetric coefficient of thermal expansion of the fluid; Ω is the rotational (angular) velocity of the fluid; ν is the kinematic viscosity of the fluid; T_w denotes the wall temperature at the plate and T_∞ the ambient temperature in the free stream. The above Eqs (1) to (4), are highly coupled and nonlinear. An analytical solution is intractable and to simplify a numerical solution we transform the system into a pseudo-similar dimensionless set of partial differential equations. Introducing the transformations:

$$X=\frac{x}{L}\,, \tag{8}$$

$$Z=\frac{z}{LGr_L^{-1/4}}\,, \tag{9}$$

$$U=\frac{uL}{\nu\mathrm{Gr}_L^{1/2}}\,, \tag{10}$$

$$V=\frac{vL}{\nu\mathrm{Gr}_L^{1/2}}\,, \tag{11}$$

$$W=\frac{wL}{\nu\mathrm{Gr}_L^{1/4}}\,, \tag{12}$$

$$K=\frac{K^*\mathrm{Gr}_L^{1/2}}{L^2}\,, \tag{13}$$

$$C=C^*L, \tag{14}$$

$$\mathrm{Pr} = \frac{\nu}{\alpha_e}\,, \tag{15}$$

$$S = \frac{aL}{T_w - T_0}\,, \tag{16}$$

$$T_\infty = T_0 + ax, \qquad \text{where} \qquad a > 0, \tag{17}$$

$$\theta = \frac{T - T_\infty}{T_w - T_0}\,, \tag{18}$$

$$\mathrm{Gr}_L = \frac{g\beta[T_w - T_0]L^3}{\nu^2}\,, \tag{19}$$

$$\mathrm{Ro} = \frac{\Omega L^2 \mathrm{Gr}_L^{1/2}}{\nu}\,, \tag{20}$$

$$a = \frac{dT_\infty}{dx}\,. \tag{21}$$

Here a is a gradient of ambient temperature $(\mathrm{K/m})$. With these transformations we obtain the following dimensionless boundary layer equations now in two independent variables (X, Z):

Conservation of Mass:

$$\frac{\partial U}{\partial X} + \frac{\partial W}{\partial Z} = 0. \tag{22}$$

Momentum:

$$\varepsilon^{-1}\left[U\frac{\partial U}{\partial X} + W\frac{\partial U}{\partial Z} - 2\mathrm{Ro}V\right] = \varepsilon^{-1}\frac{\partial^2 U}{\partial Z^2} - K^{-1}U - CU^2 + \theta, \tag{23}$$

$$\varepsilon^{-1}\left[U\frac{\partial V}{\partial X} + W\frac{\partial V}{\partial Z} + 2\mathrm{Ro}U\right] = \varepsilon^{-1}\frac{\partial^2 V}{\partial Z^2} - K^{-1}V - CV^2. \tag{24}$$

Energy (Heat):

$$U\frac{\partial \theta}{\partial X} + W\frac{\partial \theta}{\partial Z} + SU = \frac{1}{\mathrm{Pr}}\frac{\partial^2 \theta}{\partial Z^2}\,. \tag{25}$$

The boundary conditions are also transformed into:

$$U(X,0) = V(X,0) = W(X,0) = 0, \qquad \theta(X,0) = 1 - SX, \tag{26}$$

$$U(X,\infty) = V(X,\infty) = \theta(X,\infty) = 0, \tag{27}$$

$$U(0,Z) = V(0,Z) = \theta(0,Z) = 0, \qquad Z > 0, \tag{28}$$

where U, V and W are the dimensionless X, Y and Z direction velocities respectively; S denotes the dimensionless thermal stratification parameter; ε is the porosity of the porous medium; Ro is the Rossby rotational number; Gr_L is the Grashof buoyancy parameter; θ is dimensionless temperature;

L is a scale length; Pr is the Prandtl number; C is dimensionless Forcheimmer (inertial) parameter; K is the dimensionless permeability (hydraulic conductivity) of the porous medium; a is a non-isothermal parameter. In the absence of rotation of the fluid, ($\mathrm{Ro} = 0$), and the transport Eqs (22), (23) and (25) reduce to those of Chen and Lin [25] viz:

Conservation of Mass:

$$\frac{\partial U}{\partial X} + \frac{\partial W}{\partial Z} = 0\,. \tag{29}$$

Momentum:

$$\varepsilon^{-1}\left[U\frac{\partial U}{\partial X} + W\frac{\partial U}{\partial Z}\right] = \varepsilon^{-1}\frac{\partial^2 U}{\partial Z^2} - K^{-1}U - CU^2 + \theta\,. \tag{30}$$

Energy (Heat):

$$U\frac{\partial \theta}{\partial X} + W\frac{\partial \theta}{\partial Z} + SU = \frac{1}{\mathrm{Pr}}\frac{\partial^2 \theta}{\partial Z^2}\,. \tag{31}$$

We note that for $\mathrm{Ro} = 0$, Eq. (24) is not required since $V(X, Z) = 0$.

2. Numerical Solution by Blottner Difference Scheme

The governing equations amount to a seventh order set of nonlinear, coupled partial differential equations with seven corresponding boundary conditions. The Blottner method [26] has been used in a wide range of thermal convection and fluid mechanics problems. Chamkha [27] studied the natural convection due to solar radiation in porous media using the Blottner scheme. Bég et al [28] recently applied Blottner's method to investigate the unsteady hydromagnetic rotational thermal convection from a spinning sphere with strong buoyancy forces. In this method the partial derivatives are replaced by two-point backward difference approximations. The first order derivatives with respect to X are replaced by a two-point backward difference formula, as follows:

$$\frac{\partial R}{\partial X} = \frac{R_{m,n} - R_{m-1,n}}{\Delta X}\,, \tag{32}$$

where R denotes the dependent variable (U, V, or θ); m and n denote node locations in the X and Z directions. The finite difference mesh is illustrated in Fig. 2 below.

The second-order partial differential equations for U, V and θ are discretized by employing the three-point central difference formulae and the first order equations are discretized by using the

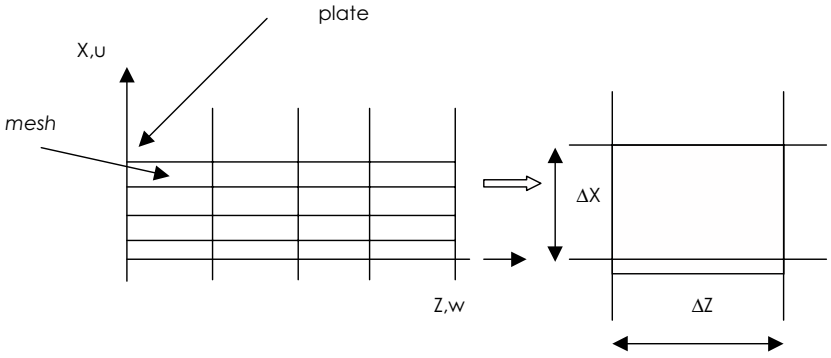

Fig. 2. XZ grid meshing and a Blottner computational cell.

trapezoidal rule . At each line of constant X we obtain a system of algebraic equations. We evaluate the nonlinear terms in the equations at the previous iteration and solve the system of algebraic equations iteratively using the Thomas algorithm. The same procedure is followed for the next X value and the equations are solved line by line until the desired X value is reached. A convergence criterion is utilized based on the relative divergence between the current and previous iterations. When this divergence attains a value of 0.00001 the solution is assumed to have reached convergence and the iterations are automatically terminated. More details of the numerics are to be found in [26]. The grid size, ΔX by ΔZ has also been varied. For grid size less than 60 by 100 the numerical values differ only in the fourth decimal place. This corresponds to an error of less than $0.5\ \%$. For the present computations we have used a grid size of 12×200. While solutions have been provided for velocities U, V, W and temperature θ, we have also computed X-direction skin friction and Y-direction skin friction and also Nusselt number functions for the heat transfer rate at the wall. These are defined as:

$$C_{fx} = \frac{\mu[\partial u/\partial z]_{z=0} L^2}{\rho \nu^2 \mathrm{Gr}_L} = \mathrm{Gr}_L^{-1/4} \frac{\partial U(X,0)}{\partial Z}\,, \tag{33}$$

$$C_{fy} = \frac{\mu[\partial v/\partial z]_{z=0} L^2}{\rho \nu^2 \mathrm{Gr}_L} = \mathrm{Gr}_L^{-1/4} \frac{\partial V(X,0)}{\partial Z}\,, \tag{34}$$

$$\mathrm{Nu} = \frac{-x[\partial T/\partial z]_{z=0}}{T_w - T_\infty} = -\mathrm{Gr}_L^{-1/4} \frac{X}{1-SX} \frac{\partial \theta(X,0)}{\partial Z}\,, \tag{35}$$

$$\mathrm{Gr}_L^{-1/4} \overline{\mathrm{Nu}} = -\int_0^1 \frac{X}{1-SX} \frac{\partial \theta(X,0)}{\partial Z} dX, \tag{36}$$

where $\overline{\mathrm{Nu}}$ is the mean Nusselt number. In order to assess the accuracy of the present computations we have compared average Nusselt numbers for the case of $\mathrm{Ro} = 0$ with those of Chen and Lin [25] and found them to be in excellent agreement. For brevity we do not reproduce the comparisons here.

3. Results and Discussion

We have computed profiles for all three components of velocity, U, V, and W, and also θ versus Z coordinate, in the Figs 3 to 6. Here $\mathrm{Ro} = 0.5$, $K = X = 1$, $C = 10$, $\mathrm{Pr} = 5.4$ (industrial solutions), $\varepsilon = 0.9$ (high porosity). The value of S i. e., thermal stratification parameter is varied from zero to 0.8. The parameter Ro measures the relative importance of the rotational force (Coriolis) and the inertial force and a value of 0.5 implies weak rotation. Generally an increase in the thermal stratification parameter, S, reduces the momentum and thermal boundary layers. Consequently the velocities in the X and Y directions (U, V) decrease with a rise in S. The velocity component in the Z direction, W is negative for $S < 0.2$ and is positive for $S > 0.2$. This implies that the axial velocity W is directed towards the plate for $S < 0.2$ (inflow) and away from it for $S > 0.2$ (outflow). The velocity components tend U and V to zero exponentially at the edge of the boundary layer ($Z \to \infty$) for all S. The temperature, θ, in the absence of stratification ($S = 0$) also decays to zero as $Z \to \infty$ in an exponential manner, but for $S \geq 0.2$ the decay is algebraic. Algebraic decay in the boundary layer has been observed by Brown and Stewartson [29] and also Kuiken [30]. Temperature θ decreases everywhere (except at $X = 0$) as S increases, since

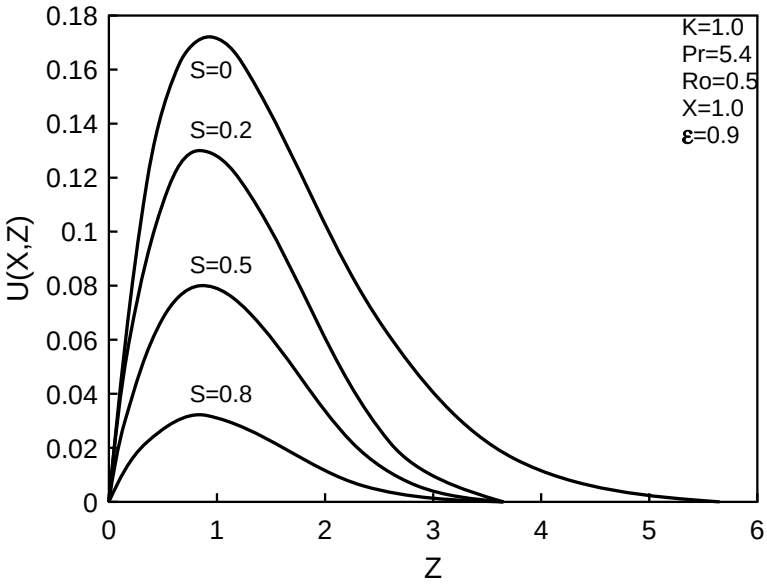

Fig. 3. Effects of S on $U(X, Z)$.

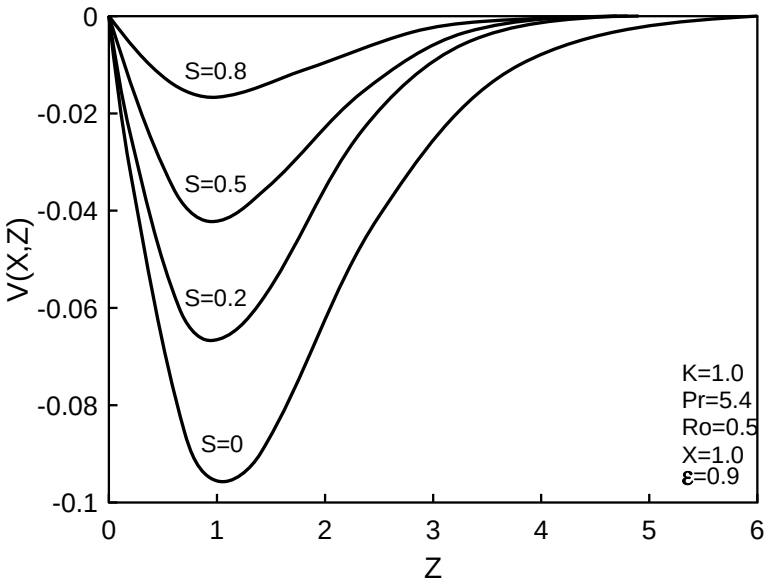

Fig. 4. Effects of S on $V(X, Z)$.

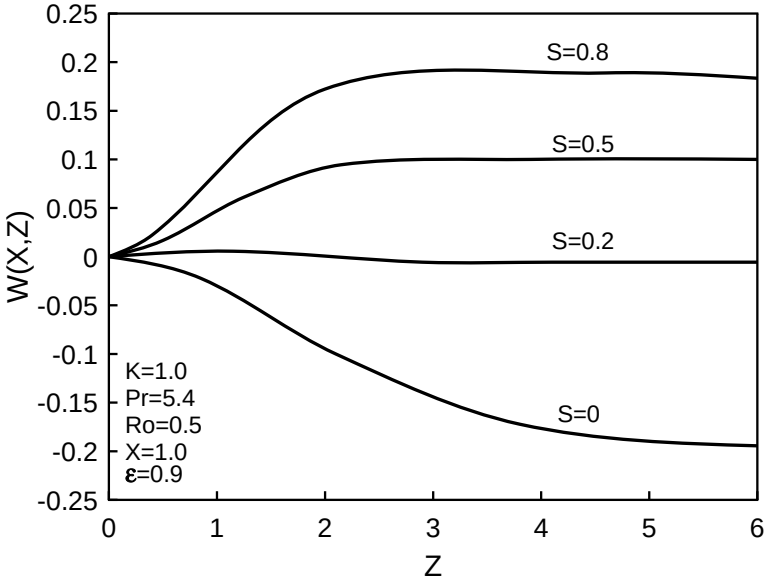

Fig. 5. Effects of S on $W(X, Z)$.

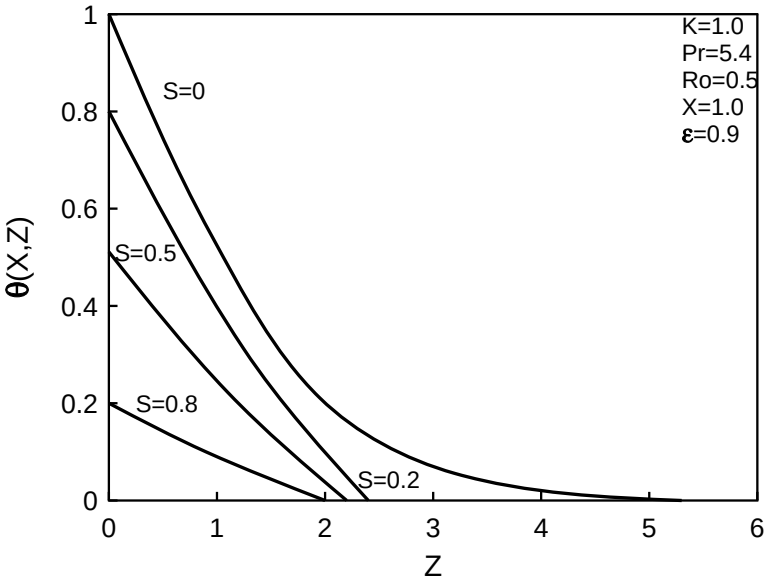

Fig. 6. Effects of S on $\theta(X, Z)$.

an increase in S also implies a reduction in the wall temperature. Thus the thermal stratification exerts a strong influence on the velocity and temperature profiles.

The variation of X and Y direction skin friction parameters, $C_{fx}\mathrm{Gr}_L^{1/4}$ and $C_{fy}\mathrm{Gr}_L^{1/4}$ respectively, against X coordinate for various thermal stratification parameter S values are plotted in Figs 7 and 8. In both cases an X range of 1.0 was found to be more than adequate for convergent solutions. The effects of stratification become more pronounced as X increases, since S is multiplied by the X variable in the boundary conditions and also by U in the heat conservation (energy) equation. Momentum and thermal boundary layers again decrease in thickness with an increase in S. We observe that for $S < 0.2$, both the X-direction and Y-direction skin friction coefficients rise with X increasing; however for $S > 0.2$, the values increase initially and then decrease. This trend is attributable to the competition between various parameters.

Fig. 9 depicts $\mathrm{Gr}_L^{-1/4}\mathrm{Nu}$ variation with X coordinate for various S values. This parameter embodies the local heat transfer rate as defined by the Nusselt number Nu. As S is increased from 0 to 0.8 the $\mathrm{Gr}_L - 1/4\mathrm{Nu}$ parameter increases in magnitude. Hence we deduce that the thermal stratification phenomenon boosts heat transfer rates at the wall.

Figs 10 to 16 illustrate the effect of the rotational parameter, Rossby number (Ro) on the all the velocity and temperature variables for the flow scenario i. e., U, V, W, θ versus Z. Parameter values are specified as $K = 1.0$, $C = 10$, $\mathrm{Pr} = 5.4$, $S = 0.5$, $X = 1.0$ and porosity $\varepsilon = 0.9$.

Since the Rossby number gives rise to a secondary flow ($V = 0$ for $\mathrm{Ro} = 0$) the secondary flow velocity V increases with Ro. Generally however the primary flow velocities (U, W) decrease. For $\mathrm{Ro} > 0.5$, flow reversal occurs in the X-component of velocity i. e., U over a certain range of Z. Also Rossby number boosts the growth of the momentum and thermal boundary layers. As a result the temperature θ also increases with Ro. The temperature profiles illustrate algebraic decay, which has been discussed earlier.

In Figs 14 to 16 we have presented plots of skin friction parameters and local heat transfer rate, viz, $C_{fx}\mathrm{Gr}_L^{1/4}$, $C_{fy}\mathrm{Gr}_L^{1/4}$ and $\mathrm{Gr}_L^{-1/4}\mathrm{Nu}$ against X coordinate for various Ro values. For these plots $K = 1.0$, $C = 10$, $\mathrm{Pr} = 5.4$, $S = 0.5$ and porosity $\varepsilon = 0.9$. The effect of the Rossby number (which is raised from 0.1 to 1.5) on all three parameters ($C_{fx}\mathrm{Gr}_L^{1/4}$, $C_{fy}\mathrm{Gr}_L^{1/4}$ and $\mathrm{Gr}_L^{-1/4}\mathrm{Nu}$) is more pronounced away from the leading edge of the plate. $C_{fx}\mathrm{Gr}_L^{1/4}$ and $\mathrm{Gr}_L^{-1/4}\mathrm{Nu}$ decrease with rising Ro; conversely $C_{fy}\mathrm{Gr}_L^{1/4}$ increases with an increase in the Rossby parameter. This is due to the growth of the secondary flow with increasing Ro values. Since Ro opposes the motion in the X direction (term $-2\mathrm{Ro}V$ in Eq. (23)) the skin friction in this direction is reduced by rising Ro values. Ro aids motion in the Y direction (term $+2\mathrm{Ro}U$ in Eq. (24)) and therefore boosts Y direction skin friction values. For a fixed Ro, $C_{fx}\mathrm{Gr}_L^{1/4}$ and $C_{fy}\mathrm{Gr}_L^{1/4}$ first increase with X, then decrease, whereas $\mathrm{Gr}_L^{-1/4}\mathrm{Nu}$ continuously increases with X.

Finally in Figs 17 and 18 we have plotted $\mathrm{Gr}_L^{-1/4}\mathrm{Nu}$ variation with X coordinate for different porosity values (ε) and different permeability parameters (K). In Fig. 17, $K = 1.0$, $C = 10$, $\mathrm{Pr} = 5.4$, $S = \mathrm{Ro} = 0.5$ and the profile shows that as ε is increased from 0.5 to 0.7 and then to 0.9 (very high) the $\mathrm{Gr}_L^{-1/4}\mathrm{Nu}$ function increases in magnitude i. e., heat transfer rates are boosted for higher porosities as the relative dominance of convection heat transfer to conduction heat transfer is greater as the medium tends to a more porous one. For lower porosities more solid particles are present leading to greater heat transfer by conduction and lesser transport by the convection mode. In the limit of $\varepsilon \to 1$, the medium is pure fluid as all the solid particles in the porous matrix would cease to exist for this case. Less resistance is experienced by the fluid with rising porosity and the fluid accelerates therefore with increasing porosity. This extracts more heat from the plate surface

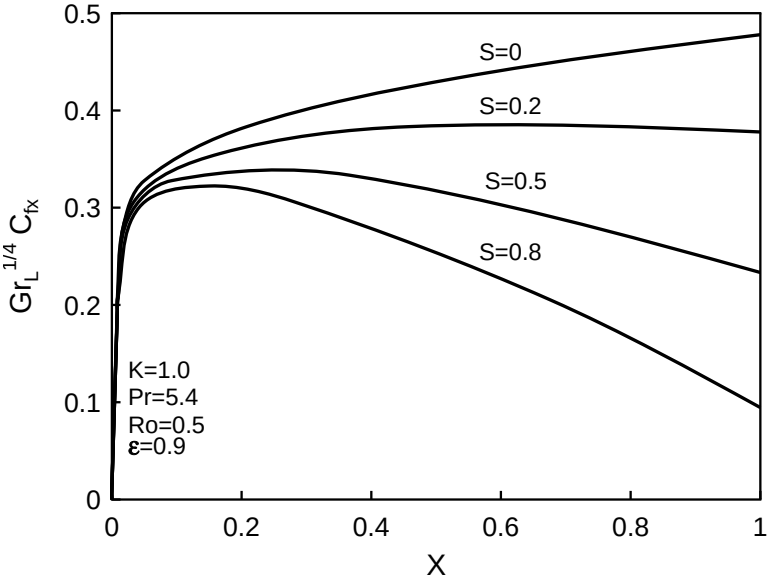

Fig. 7. Effects of S on $\mathrm{Gr}_L^{1/4} C_{fx}$.

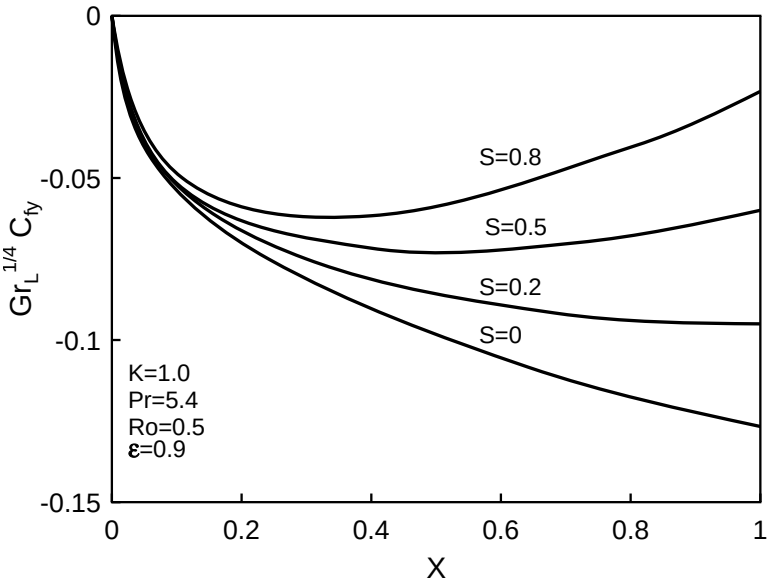

Fig. 8. Effects of S on $\mathrm{Gr}_L^{1/4} C_{fy}$.

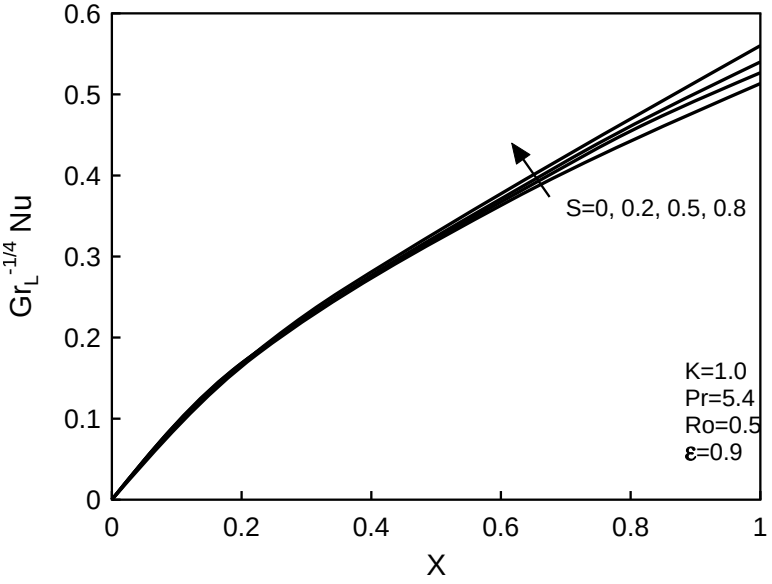

Fig. 9. Effects of S on $\mathrm{Gr}_L^{1-/4}\mathrm{Nu}$.

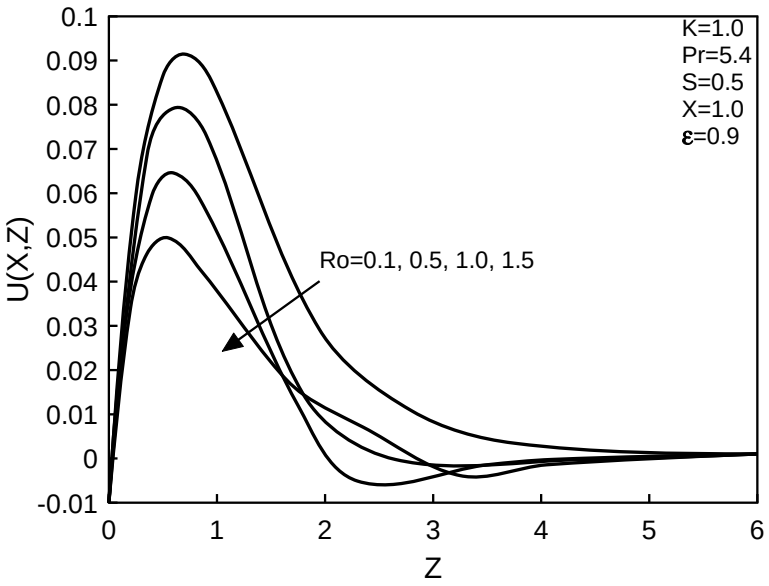

Fig. 10. Effects of Ro on $U(X, Z)$.

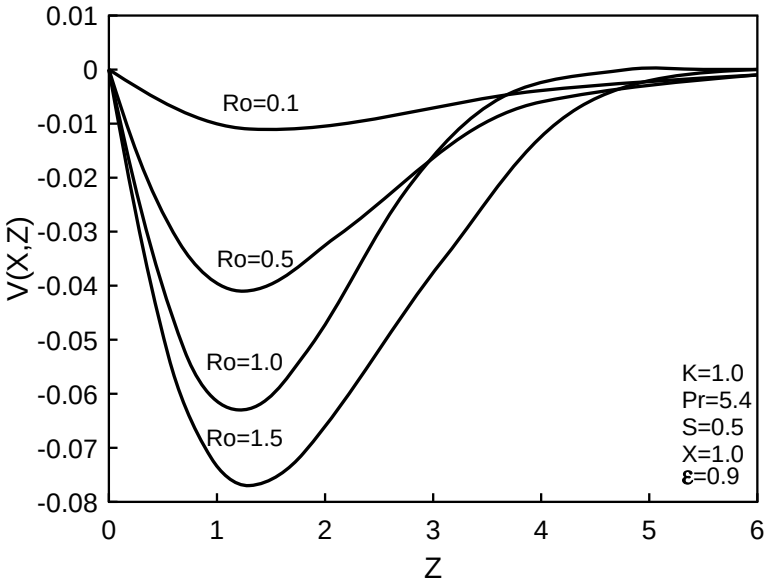

Fig. 11. Effects of Ro on $V(X, Z)$.

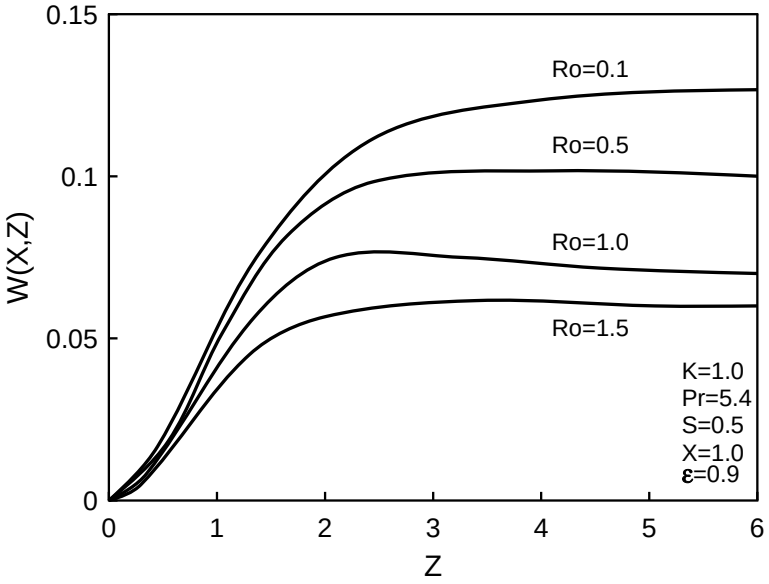

Fig. 12. Effects of Ro on $W(X, Z)$.

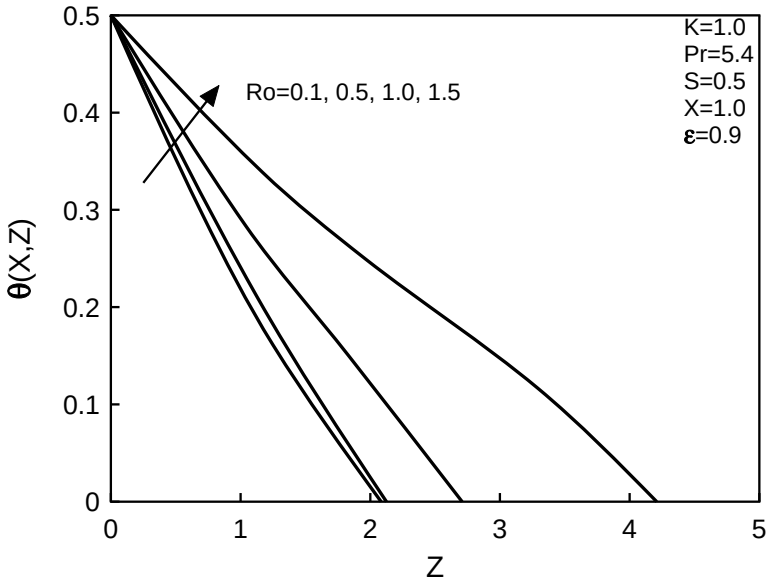

Fig. 13. Effects of Ro on $\theta(X, Z)$.

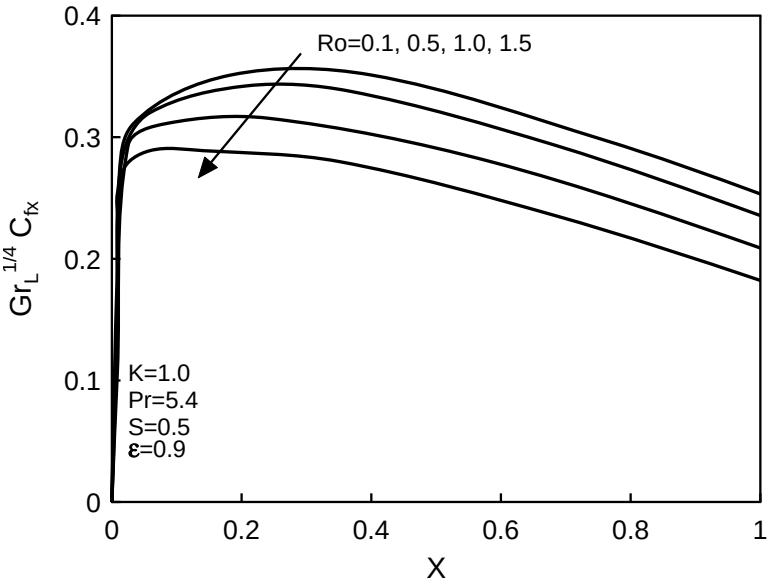

Fig. 14. Effects of Ro on $\mathrm{Gr}_L^{1/4} C_{fx}$.

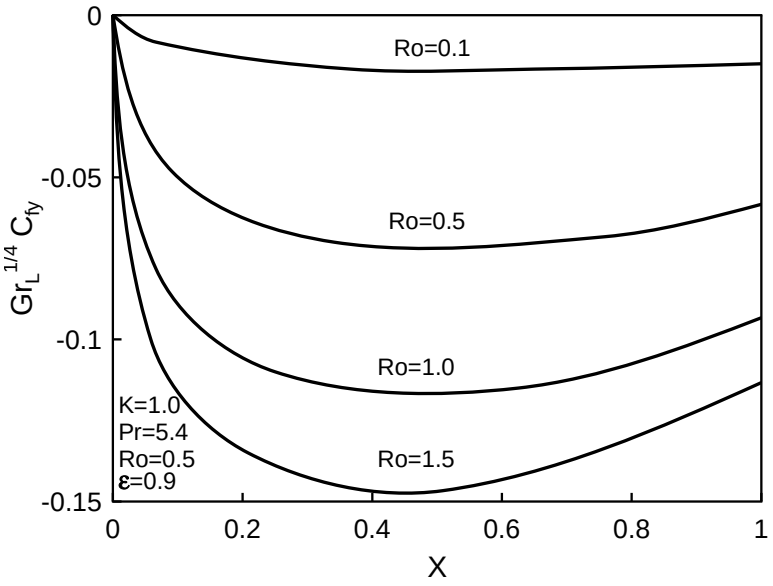

Fig. 15. Effects of Ro on $\mathrm{Gr}_L^{1/4} C_{fy}$.

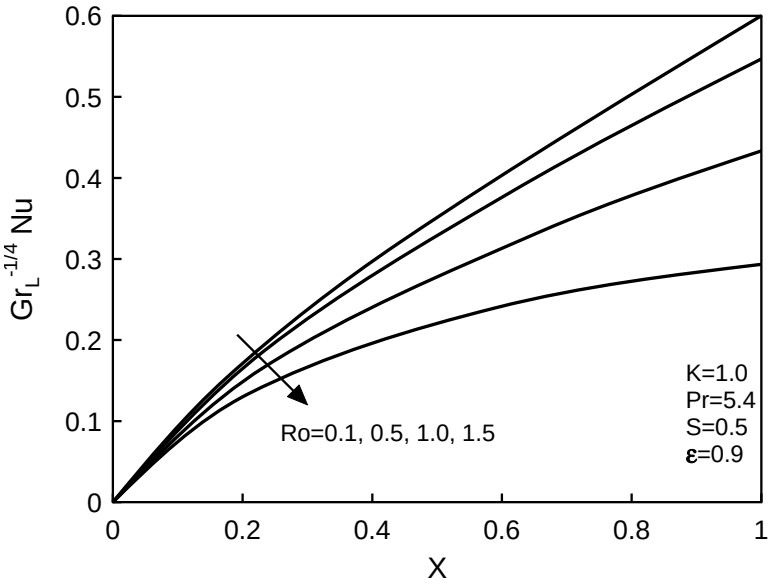

Fig. 16. Effects of Ro on $\mathrm{Gr}_L^{1-/4}\mathrm{Nu}$.

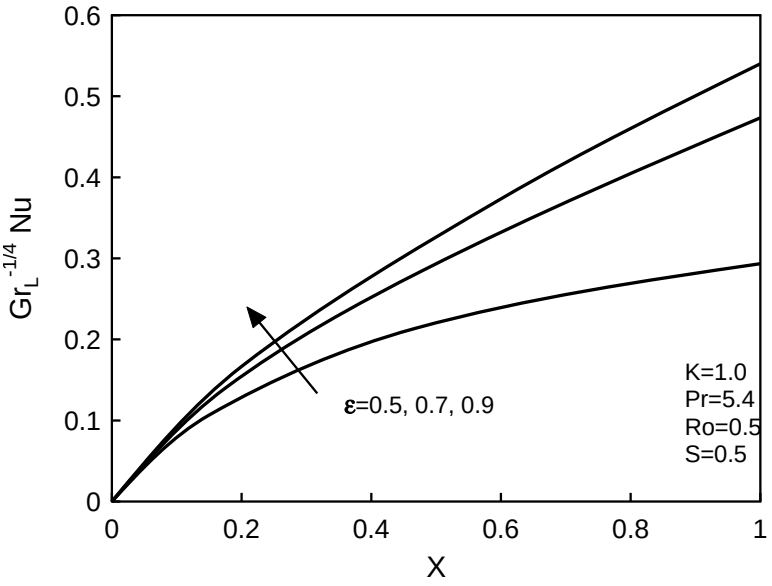

Fig. 17. Effects of ε on $\mathrm{Gr}_L^{1-/4}\mathrm{Nu}$.

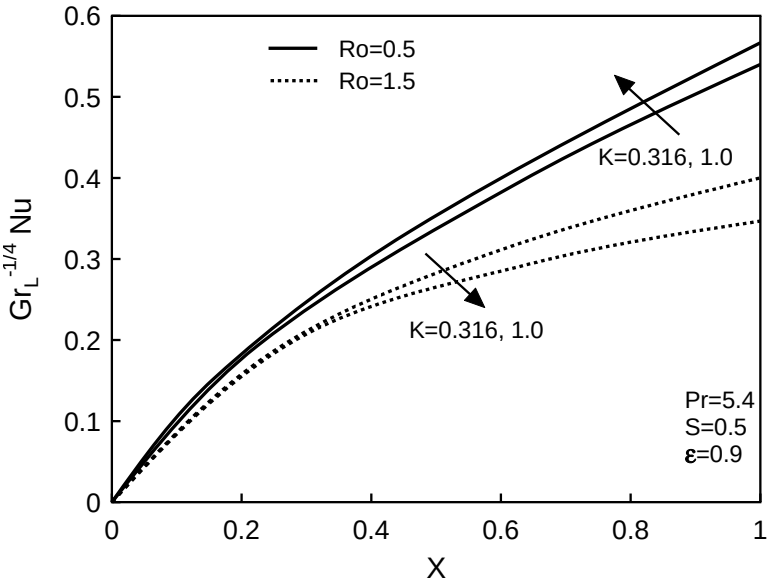

Fig. 18. Effects of K on $\mathrm{Gr}_L^{1-/4}\mathrm{Nu}$.

and consequently the thermal boundary layer thickness decreases and Nusselt number is enhanced. Porosity has a strong influence on the Nusselt number function which increases by about $95\ \%$ as porosity ε rises from 0.5 to 0.9. Fig. 18 illustrates two sets of profiles, one for $\mathrm{Ro} = 0.5$ and the other for $\mathrm{Ro} = 1.5$, with other parameter values fixed at $\mathrm{Pr} = 5.4$, $S = 0.5$, $C = 10$, $\varepsilon = 0.9$. $\mathrm{Gr}_L^{-1/4}\mathrm{Nu}$ function plotted against X is seen increase with rising K (0.316 to 1.0) for $\mathrm{Ro} = 0.5$ i. e., with lower rotational strengths the heat transfer at the wall is elevated with higher permeabilities. An increase in K implies physically less resistance to the fluid motion by the porous medium which generates a thinner thermal boundary layer. For the case of $\mathrm{Ro} = 1.5$ the trend is reversed since the thermal boundary layer grows more rapidly with the boost from rotation, compared with the reduction induced by an increase in K, i. e., the overall effect is a positive one where rotation rise dominates permeability effects. Hence we can deduce that the heat transfer rate i. e., Nusselt number function, $\mathrm{Gr}_L^{-1/4}\mathrm{Nu}$, has a weak dependence on K. It increases by about $4\ \%$ as permeability K is increased from 0.316 to 1.0, when $\mathrm{Ro} = 0.5$.

Finally we note that the Nusselt number function $\mathrm{Gr}_L^{-1/4}\mathrm{Nu}$, decreases with increasing inertial parameter, C, since the momentum and thermal boundary layers become thick due to an increase in the resistance to motion. For $\mathrm{Pr} = 5.4$, $\mathrm{Ro} = S = 0.5$, $\varepsilon = 0.9$, $K = X = 1$, $\mathrm{Gr}_L - 1/4\mathrm{Nu}$, increases by approximately $35\ \%$ as C rises from 0 to 200. For lower Prandtl numbers a lower percentage increase in $\mathrm{Gr}_L^{-1/4}\mathrm{Nu}$ has been computed (the graphs are not shown here for brevity).

Conclusions

The convective heat transfer flow in a rotating fluid over a vertical plate in a thermally-stratified high-porosity medium has been examined numerically. It has been shown that thermal stratification of the fluid (S), Rossby number (Ro) and porosity of the composite medium (ε) exert a strong influence on the velocity and temperature fields. X-direction skin friction and Nusselt number function are shown to increase with thermal stratification parameter,with the converse apparent i. e., a decrease in Y-direction skin friction. The effects of the Rossby number are poosite to those of the stratification parameter, S. Temperature θ profiles in the presence of thermal stratification decay to zero at the edge of the boundary layer algebraically whereas the velocity profiles (U, V, W) tend to their asymptotic values at the edge of the boundary layer exponentially. Beyond a critical value of the Rossby number ($\mathrm{Ro} \geq 0.5$) flow reversal occurs in the X-component of the velocity. The present results are of importance in various chemical and geophysical flow regimes. At present the first three authors of this paper, are extending the present model to consider electrohydrodynamic effects of pertinence in various electronic and energy generation systems. Results will be reported in the future [31].

REFERENCES

1. Lyttleton, R. A., *Theory of Rotating Fluid Masses*, Cambridge University Press, Cambridge, England, 1953.
2. Greenspan, H. P., *The Theory of Rotating Fluids*, Cambridge University Press, New York, 1968.
3. Dorfman, L. A., *Hydrodynamic Resistance and the Heat Loss of Rotating Solids*, Oliver & Boyd, Edinburgh, 1963.
4. Kreith, F. , Convection Heat Transfer in Rotating Systems, In: *Advances in Heat Transfer*, Vol. 5, Academic Press, New York, 1968, pp. 129–151.

5. Rotem, Z. and Classen, L., In: *4th International Heat Transfer Conference*, Versailles, **IV**Pap. NC4.3, 1970.
6. Suwono, A., Buoyancy Effects on Flow and Heat Transfer on Rotating Axisymmetric Round-Nosed Bodies, *Int. J. Heat Mass Transfer*, 1980, **23**, No. 6, pp. 819–831.
7. Takhar, H. S. and Whitelaw, M. H., Higher Order Heat Transfer from a Rotating Sphere, *Acta Mechanica*, 1978, **30**, pp. 101–109.
8. Hossain, M. A. and Takhar, H. S., Radiation-Conduction Interaction in Mixed Convection on Rotating Bodies, *Heat Mass Transfer. Wärme- und Stoffübertragung*, 1997, **33**, pp. 201–208.
9. Naroua, H., Ram, P. C., Sambo, A. S., and Takhar, H. S., Finite Element Analysis of Natural Convection Flow in a Rotative Fluid with Radiative Heat Transfer, *J. Magnetohydrodyn. Plasma Resch*, 1998, **7**, pp. 257–274.
10. Deka, R. K., Gupta, A. S., Takhar. H. S., and Soundalgekar, V. M., Flow Past an Accelerated Horizontal Plate in a Rotating Fluid, *Acta Mechanica*, 1999, **30**, pp. 594–600.
11. Pop, I., Soundalgekar, V. M., and Takhar, H. S., Dispersion of a Soluble Matter in a Porous Medium Channel with Homogenous and Heterogenous Chemical Reaction, *Revue Romanie. Mecanique Appliquee*, 1983, **28**, pp. 127–132.
12. Takhar. H. S., Soundalgekar, V. M., and Singh, M., Unsteady Flow in Porous Medium Between Two Infinite Parallel Plates in Relative Motion, *Trans. ASME. J. Fluids Engng*, 1985, **107**, pp. 534–535.
13. Raptis, A. A. and Takhar, H. S., Combined Mass Transfer and Forced Flow Through a Porous Medium, *Int. Comm. Heat Mass Transfer*, 1986, **13**, pp. 599–603.
14. Takhar., H. S. and Pop, I., Free Convection from a Vertical Flat Plate to a Thermally Stratified Darcian Flow, *Mech. Resch Comm.*, 1987, **14**, pp. 81–86.
15. Vafai, K. and Tien, C. L., Boundary and Inertia Effects on Flow and Heat Transfer in Porous Media, *Int. J. Heat Mass Transfer*, 1981, **24**, pp. 195–203.
16. Kumari, M., Takhar., H. S., and Nath, G., Double Diffusive Non-Darcy Free Convection from Two-Dimensional and Axi-Symmetric Bodies of Arbitrary Shape in a Saturated Porous Medium, *Indian J. Technol.*, 1988, **26**, pp. 324–328.
17. Kumari, M., Takhar, H. S., and Nath, G., Non-Darcy Double-Diffusive Mixed Convection from Heated Vertical and Horizontal Plates in Saturated Porous Media, *Thermo-Fluid Dynamics. Wärme -und Stoffübertragung*, 1988, **23**, pp. 267–273.
18. Takhar, H. S., Soundalgekar, V. M., and Gupta, A. S., Mixed Convection of an Incompressible Fluid in a Porous Medium Past a Hot Vertical Plate, *Int. J. Non-Linear Mech.*, 1990, **25**, pp. 723–728.
19. Gorla, R. S. R. and Takhar, H. S., Combined Convective Heat Transfer from a Plate Embedded in Porous Media, *Int. J. Engng Fluid Mech.*, 1991, **4**, pp. 363–373.
20. Takhar, H. S. and Bég, O. A., Effects of Transverse Magnetic Field, Prandtl Number and Reynolds Number on Non-Darcy Mixed Convection Flow of an Incompressible Viscous Fluid Past a Porous Flat Plate in a Saturated Porous Medium, *Int. J. Energy Resch*, 1997, **21**, pp. 87–100.
21. Takhar, H. S., Bég, O. A., and Kumari, M., Computational Analysis of Coupled Radiation-Convection Dissipative Non-Gray Gas Flow in a Non-Darcy Porous Medium Using the Keller-Box Implicit Difference Scheme, *Int. J. Energy Resch*, 1998, **22**, pp. 141–159.
22. Bég, O. A., Takhar, H. S., Soundalgekar, V. M., and Woo, G. Hydrodynamic and Heat Transfer Modelling of a Viscoelastic (Oil Spill) Flowing Through Geomaterial with Boundary Vorticity Effects. Numerical Simulation, In: *2nd Int. Conf. on Computational Heat and Mass Transfer*, Rio De Janeiro, Brazil, October 22–26, 2001.
23. Takhar, H. S., Chamkha, A. J., and Nath. G., Natural Convection on a Vertical Cylinder Embed-

ded in a Thermally Stratified High-Porosity Medium, *Int. J. Thermal Sci.*, 2002, **41**, pp. 83–93.
24. Tien, C. L. and Vafai, K., Convective and Radiative Heat Transfer in Porous Media, *Adv. Appl. Mech.*, 1989, **27**, pp. 225-281.
25. Chen, C. K. and Lin, C. R., Natural Convection from an Isothermal Vertical Surface Embedded in a Thermally-Stratified High-Porosity Medium, *Int. J. Engng Sci.*, 1995, **33**, pp. 131–138.
26. Blottner, F. G., Finite Difference Method of Solution of the Boundary Layer Equations, *Amer. Inst. Aeronaut. Astronaut. J.*, 1970, **8**, pp. 193.
27. Chamkha, A. J., Solar Radiation Assisted Natural Convection in a Uniform Porous Medium Supported by a Vertical Flat Plate, *ASME J. Heat Transfer*, 1997, **119**, pp. 35–43.
28. Takhar, H. S., Bég, O. A., and Chamkha, A. J. Mathematical Modelling of Hydromagnetic Convection from a Rotating Sphere with Impulsive Motion and Buoyancy, In *WSEAS/ASME Int. Conf. on Heat and Mass Transfer*, Corfu, Greece, August, 2004.
29. Brown, S. N. and Stewartson, K., On Similarity Solutions of the Boundary Layer Equations with Algebraic Decay, *J. Fluid Mechanics*, 1965, **23**, pp. 673–687.
30. Kuiken, H. K., On Boundary Layers in Fluid Mechanics that Decay Algebraically Along Stretches of Wall that are Non-Vanishingly Small, *IMA J. Appl. Math.*, 1981, **27**, pp. 387–405.
31. Takhar, H. S, Bég, O. A., and Bég, T. A., Electrohydrodynamic Convection Heat Transfer in Porous Media, *Acta Mechanica*, May, 2006 [in preparation].

□◆◆◆□